HHS Public Access

Author manuscript

Cancer Res. Author manuscript; available in PMC 2017 March 01.

Published in final edited form as:

Cancer Res. 2016 March 1; 76(5): 999–1008. doi:10.1158/0008-5472.CAN-15-1439.

STK11/LKB1 deficiency promotes neutrophil recruitment and proinflammatory cytokine production to suppress T cell activity in the lung tumor microenvironment

Shohei Koyama[1,2,*], **Esra A. Akbay**[2,3,*], **Yvonne Y. Li**[2,3,*], **Amir R. Aref**[2,3], **Ferdinandos Skoulidis**[4], **Grit S. Herter-Sprie**[2,3], **Kevin A. Buczkowski**[3], **Yan Liu**[2,3], **Mark M. Awad**[2,3], **Warren L. Denning**[4], **Lixia Diao**[5], **Jing Wang**[5], **Edwin R. Parra-Cuentas**[6], **Ignacio I. Wistuba**[6], **Margaret Soucheray**[7], **Tran C. Thai**[3], **Hajime Asahina**[2,3], **Shunsuke Kitajima**[3], **Abigail Altabef**[3], **Jillian D. Cavanaugh**[3], **Kevin Rhee**[3], **Peng Gao**[3], **Haikuo Zhang**[2,3], **Peter E. Fecci**[8], **Takeshi Shimamura**[9], **Matthew D. Hellmann**[10], **John V. Heymach**[4], **F. Stephen Hodi**[2,3], **Gordon J. Freeman**[1,2], **David A. Barbie**[2,3], **Glenn Dranoff**[11,**], **Peter S. Hammerman**[2,3,**], and **Kwok-Kin Wong**[2,3,12,**]

[1]Department of Medical Oncology and Cancer Vaccine Center, Dana Farber Cancer Institute, Boston, MA

[2]Department of Medicine, Brigham and Women's Hospital and Harvard Medical School, Boston MA

[3]Department of Medical Oncology, Dana Farber Cancer Institute, Boston MA

[4]Department of Thoracic/Head and Neck Medical Oncology, The University of Texas MD Anderson Cancer Center, Houston, Texas

[5]Department of Bioinformatics and Computational Biology, The University of Texas MD Anderson Cancer Center, Houston, Texas

[6]Department of Translational Molecular Pathology, The University of Texas MD Anderson Cancer Center, Houston, Texas

[7]University of California San Francisco

[8]Division of Neurosurgery, Department of Surgery, Duke University Medical Center, Durham, North Carolina

[9]Department of Molecular Pharmacology and Therapeutics, Oncology Research Institute, Loyola University Chicago, Illinois

[10]Department of Medicine, Memorial Sloan Kettering Cancer Center, New York, NY

[**]Address correspondence to: Kwok-Kin Wong, kwong1@partners.org, phone: 617-582-7683, and fax: 617-582-7839, Peter Hammerman, peter_hammerman@dfci.harvard.edu, phone: 617-632-3647, and fax: 617-632-5786, or Glenn Dranoff glenn.dranoff@novartis.com, phone: 617 871 4700.

[*]These authors equally contributed to this work

Disclosure of Potential Conflicts of Interest:

G.D. received sponsored research support from Bristol-Myers Squibb and Novartis, and is currently an employee of Novartis. He is currently an employee of Novartis. G.J.F. receives patent royalties on the PD-1 pathway from Bristol-Myers-Squibb, Roche, Merck, EMD-Serrono, Boehringer-Ingelheim, Amplimmune/AstraZeneca, and Novartis. F.S.H. is a Bristol-Myers Squibb nonpaid consultant, Novartis, Merck and Genentech consultant and receives clinical trial support to the institution from these companies.

[11]Novartis Institutes for BioMedical Research, Cambridge, MA

[12]Belfer Institute for Applied Cancer Science, Dana Farber Cancer Institute, Boston, MA

Abstract

STK11/LKB1 is among the most commonly inactivated tumor suppressors in non-small cell lung cancer (NSCLC), especially in tumors harboring *KRAS* mutations. Many oncogenes promote immune escape, undermining the effectiveness of immunotherapies, but it is unclear whether inactivation of tumor suppressor genes such as *STK11/LKB1* exert similar effects. In this study, we investigated the consequences of *STK11/LKB1* loss on the immune microenvironment in a mouse model of *KRAS*-driven NSCLC. Genetic ablation of *STK11/LKB1* resulted in accumulation of neutrophils with T cell suppressive effects, along with a corresponding increase in the expression of T cell exhaustion markers and tumor-promoting cytokines. The number of tumor-infiltrating lymphocytes was also reduced in *LKB1*-deficient mouse and human tumors. Furthermore, *STK11/LKB1* inactivating mutations were associated with reduced expression of PD-1 ligand PD-L1 in mouse and patient tumors as well as in tumor-derived cell lines. Consistent with these results, PD-1 targeting antibodies were ineffective against *Lkb1*-deficient tumors. In contrast, treating *Lkb1*-deficient mice with an IL-6 neutralizing antibody or a neutrophil-depleting antibody yielded therapeutic benefits associated with reduced neutrophil accumulation and proinflammatory cytokine expression. Our findings illustrate how tumor suppressor mutations can modulate the immune milieu of the tumor microenvironment, and they offer specific implications for addressing *STK11/LKB1* mutated tumors with PD-1 targeting antibody therapies.

Introduction

The discovery of a series of oncogene driver mutations and the concept of oncogene addiction has changed the therapeutic approach for subsets of patients with non-small cell lung cancers (NSCLCs) (1). While this targeted approach for tumors with specific kinase alterations has been successful, *KRAS* mutation is the most common genetic alteration driving NSCLCs and remains refractory to targeted treatment strategies. *KRAS* mutated NSCLCs are genomically more complex than those harboring mutated *EGFR* or *EML4-ALK* and the concurrent loss of key tumor suppressors such as *TP53* or *STK11* is common in *KRAS* mutated lung adenocarcinomas.

STK11/*LKB1* is inactivated in approximately one-third of *KRAS* mutated lung adenocarcinomas, a frequency comparable to *TP53* loss in this background, though *STK11* and *TP53* mutations rarely overlap in *KRAS* mutant lung tumors (2). *Lkb1*-deficient *Kras*-mutated (*Kras/Lkb1)* tumors show a more invasive and metastatic phenotype with significantly reduced survival (3) and differential drug sensitivities as compared to *Kras* mutant *Lkb1*-wild type tumors and *Kras* mutated compound *Tp53* deficient animals (4). A more metastatic phenotype in *Kras/Lkb1* tumors has also been described in clinical studies (5,6).

Recent clinical trials in NSCLC have demonstrated response to immune checkpoint blockade and nominated predictive markers for the efficacy of specific immunotherapies (7–

9). Our previous work suggests that oncogenes impact immune evading mechanisms by directly activating immune checkpoints (10). Immune evasion can also be achieved by the release of proinflammatory cytokines into the tumor microenvironment that play an important role in promoting tumor growth, metastasis and immune suppression (11,12). Previous work has shown that *Kras*-mutated tumors display activation of the non-canonical IkappaB kinase TBK1 (13,14) that activation of this signaling pathway induces several proinflammatory cytokines, such as IL-6 and CXC-chemokine ligands. Myeloid cells, especially tumor-associated macrophages (TAM) and neutrophils (TAN), support tumor cell proliferation and impede host immune surveillance through cytokine production and cell-cell interactions (15).

To elucidate how *Stk11/Lkb1* (hereafter referred to as *Lkb1* in the mouse model) -loss affects the inflammatory phenotype in *Kras*-driven lung cancer, we compared immune cell populations and cytokine/chemokine profiles among *Kras* and *Kras/Lkb1* mouse lung cancer models. We found that neutrophil attracting soluble factors and neutrophil numbers were significantly increased and both T cell numbers and function were significantly decreased in *Lkb1*-deficient tumors. Moreover, *Lkb1*-loss of function negatively impacted PD-L1 expression in lung tumor cells in mouse and human tumors and cell lines. By depleting the neutrophils in *Kras/Lkb1* mutant mice, T cell numbers and function were significantly improved affirming the immune suppressive properties of this cell type. Finally, we functionally validated the therapeutic utility of blocking the cytokine feedback loop with a neutralizing anti-IL-6 antibody, which resulted in an increase of T cell numbers and function. Together, the results suggest that in the *Lkb1*-deficient tumors, immune evasion is achieved through suppressive myeloid cells and aberrant cytokine production and not the PD-1:PD-L1 interaction.

Methods

Murine cell line and *in* vivo studies

Mouse strains were described previously (3). Mice were dosed with 200 micrograms of IL-6 neutralizing antibody (MP5-20F3, BioXcell), anti Ly-6G/Gr-1 antibody (RB6-8C5, BioXcell), PD-1 blocking antibody (clone 29F.1A12) and isotype controls (BioXcell) three times a week via intraperitoneal injections. MRI quantification was performed as described previously (10). Murine cell lines bearing mutated *Kras* and *p53*-loss (*Kras/p53*:KP) and mutated *Kras* and both *p53* and *Lkb1*-loss (*Kras/p53/Lkb1*:KPL) were established and characterized previously (16). Recombinant mouse IL-1α was from PeproTech.

Immune cell isolation, analysis and sorting

Lung cell isolation, mononuclear cell enrichment and characterization of immune cell populations in murine tissue samples were described previously (10). Total cell count was divided by tumor-bearing lung weight utilized for each assay. Antibodies are listed in Supplementary Methods. Intracellular staining for Ki-67, IFNγ, CTLA-4, FOXP3 and LGALS9 was performed according to the manufacturer's protocol (eBioscience and BD biosciences). Sorting of tumor cells ($CD45^{-}EpCAM^{+}$) and neutrophils

($CD45^+CD11b^+Ly\text{-}6G^+$) was performed on a BD FACS Aria II. Gating methods for immune analysis and sorting are in Supplementary Methods.

Sample preparation for RNA sequencing

RNA isolation from sorted cells was performed using the PicoPure RNA Isolation kit (Life technologies) according to the manufacturer's protocol. 10–100 ng of total RNA was used as input for the generation libraries using the Nugen Ovation Kit. Libraries were quality controlled on an Agilent high sensitivity DNA chip and sequencing of pooled libraries performed on the Illumina HiSeq platform to a minimum depth of 30 million reads.

Mouse RNA sequencing and patient tumor gene expression and proteomic data analysis (CCLE, TCGA, and PROSPECT)

Methods for these are described in supplementary methods.

Preparation of isogenic human cell lines and IL1-α stimulation

Human lung cancer cell lines were obtained from ATCC and used prior to six months of passage in culture and not further authenticated. Short hairpin RNA constructs and stable isogenic cell lines were established as described previously (17). Recombinant human IL-1α was from PeproTech (18).

Immunohistochemistry

Immunohistochemistry for TUNEL and Ki-67 was performed as previously described (19). For the PROSPECT samples 4μm- thick tissue sections were stained using an automated staining system (Leica Bond Max, Leica Microsystems, Vista, CA, USA), according to standard protocols. The38 Aperio Image Analysis Toolbox (Aperio, Leica Microsystems) was used for digital analysis of images obtained from scanned slides. PDL1 clone E1L3N from Cell Signaling Technologies, CD3 A0452 from Dako and CD8 C8/144B from Thermo Scientific were used.

Western blotting

Tumor nodules resected from *Kras* and *Kras/Lkb1* mice were homogenized in RIPA buffer and proteinase inhibitor (Cell Signaling Technology). Western blotting was performed as described previously (18) with anti pSTAT3, STAT3, LKB1 and actin antibodies (Cell Signaling Technology).

Measurement of soluble factor concentrations in BALFs from mice and culture supernatants from murine and human cell lines

Methods for these are described in supplementary methods.

Statistical analysis

All numerical data are presented as mean ± SD. Data were analyzed using two-tailed unpaired Student's *t* test for comparisons of two groups and one-way ANOVA with Tukey post-test for three groups. P values for the survival curves have been calculated using a log-rank test. Mann-Whitney U tests were used to assess correlation of PD-L1 and T cell

markers in human tumor samples with LKB1 status. Multivariate testing of TCGA data with respect to genotype and clinical factors (sex, primary tumor stage, nodal stage, metastasis stage, overall stage, age, and smoking) was performed using one-way ANOVA.

Results

Lkb1-deficient tumor cells stimulate neutrophil recruitment through the production of cytokines and chemokines

We previously showed that oncogene activation contributes to escape from immune surveillance by modulating the tumor microenvironment (10). However, the loss of tumor suppressors has not been previously investigated in this context. To elucidate how *Lkb1*-deficiency impacts the immune microenvironment in lung tumors, we compared the immune cell populations and cytokine profiles of *Kras* (K) and *Kras/Lkb1* (KL) mouse models with similar degrees of tumor burden (Supplementary Fig. S1A). We found that *Lkb1*-deficient tumors showed a greater variation in the number of total hematopoietic ($CD45^+$) cells (Supplementary Fig. S1B) and an increase in the total $CD11b^+$ myeloid cell population among three major clusters ($CD11c^-CD11b^-$, $CD11c^+CD11b^-$, $CD11b^+$) in the lung (Fig. 1A). Detailed analysis of these myeloid cell populations showed that total numbers of tumor-associated neutrophils (TAN: $CD11b^+Ly\text{-}6G^+$) are significantly elevated and tumor-associated alveolar macrophages (TAM: $CD11c^+CD11b^-CD103^-$) are significantly decreased in KL tumors compared to K tumors (Fig. 1A). Minor myeloid cell populations including eosinophils, $Ly\text{-}6C^{hi}$ inflammatory monocytes and $CD103^+$ dendritic cells did not show significant differences (Supplementary Fig. S1C). Interestingly, the increase of neutrophils was also observed in the spleen and peripheral blood of KL mice (Fig. 1B).

To identify the cytokines and chemokines driving the immune phenotype of *Lkb1*-deficient tumors, we sorted $CD45^-EpCAM^+$ cells from *Kras* and *Kras/Lkb1* lung tumors using fluorescence-activated cell sorting (FACS) and performed mRNA sequencing. We discovered higher expression of a number of chemokines in the KL tumor cells: *Ppbp* (pro-platelet basic protein: chemokine (C-X-C motif) ligand 7 (*Cxcl7*)), *Cxcl3* and *Cxcl5*, all of which act through chemokine receptor CXCR2 on neutrophils (Supplementary Methods), and cytokines: *Csf3* (Colony stimulating factor 3: granulocyte colony stimulating factor (*G-Csf*)) and two of the IL-1 family of proinflammatory cytokines; *Il33*, *Il1α* (Fig. 1C). On the contrary, we identified a decrease in the expression of chemokine (C-C motif) ligand 5 (*Ccl5*) and *Cxcl12* in KL tumor cells as compared to *Kras*. Both of these chemokines play an important role in recruiting lymphocytes and dendritic cells (20,21) and these cell types are underrepresented in KL tumors (Supplementary Fig. S1C and D).

In addition to tumor cells, we sorted TAN from KL tumors and compared gene expression profiles with TAN from the uninduced normal lung from mice with the same genetic background. Analysis of mRNA sequencing revealed that TAN from the KL tumors produced elevated T cell suppressive factors (22) including *Il10*, *Lgals9*, *Arginase 1 (Arg1)* and *Milk fat globulin EGF factor 8 protein (Mfge8)* and the tumor promoting cytokine *Il6*, as compared to neutrophils from normal lung (Supplementary Fig. 2A).

To confirm these findings at the protein level, we analyzed CXCL7, G-CSF, and IL-1α in culture supernatants from cell lines derived from mouse tumors (16). There was a significant increase in CXCL7 and G-CSF in *Kras*-mutated *Tp53*-deficient *Lkb1*-deficient cell lines (KPL) compared to *Kras*-mutated *Tp53*-deficient *Lkb1*-wild type cell lines (KP) (Fig. 1D) but IL-1α was under the detection limit in all cell lines (data not shown). In addition to the cytokines identified as differentially expressed in mRNA sequencing, we analyzed IL-6 and IL-17, two well characterized cytokines that contribute to neutrophil accumulation and production (23,24), and found that IL-6 was significantly increased in KPL compared to KP (Fig. 1D) but IL-17 was not detected (data not shown). We further evaluated the cytokines in BALFs which showed a significant increase of CXCL7 in KL versus control and G-CSF, MFG-E8, and IL-10 in KL versus control and K (Fig. 1E and Supplementary Fig. 2B). While *Il-6* upregulation was not apparent at the mRNA level in $EpCAM^+$ KL tumors cells (data not shown), we detected the cytokine in BALFs from KL lungs and in cultured sorted $CD45^-EpCAM^+$ cells and TAN from KL tumors (Supplementary Fig. 2C). Considering the higher number of neutrophils in KL tumors as compared to K tumors, TAN likely play an important role in aberrant production of this cytokine in addition to tumor cells. Given that IL-6 mediates its downstream affects through STAT3 (25) we measured levels of phosphorylated STAT3. We found that *Kras/Lkb1* tumor tissue had higher levels of phospho-STAT3 (pSTAT3) than the *Kras* tumors (Fig. 1F). These findings suggest that *Lkb1*-inactivation is associated with neutrophil accumulation to the immune microenvironment and overproduction of tumor-promoting cytokines.

In concordance with RNA sequencing data, IL-1α showed a significant increase in BALFs in *Kras/Lkb1* versus that from control (Fig. 1G). Mouse BALFs, similar to the supernatants from cultured cells, did not have detectable IL-17 (data not shown). To assess whether IL-1α might promote feed forward cytokine signaling in *Lkb1*-deficient tumors, we stimulated a *Kras*-mutated, *p53*-loss, *Lkb1*-loss mouse lung cancer cell line (KPL cell line) with IL-1α and analyzed cytokine secretion. Among the cytokines, we detected an increase in IL-6, CXCL7 and G-CSF production in a dose-dependent manner (Fig. 1H and Supplementary Fig. S3A). These results are consistent with *Lkb1*-loss increasing IL-1α production, which then promotes the activation of IL-6-STAT3 signaling.

Lkb1-loss negatively impacts the number and function of tumor infiltrating T cells and PD-L1 expression on tumor cells

Clinical studies have demonstrated that the density of tumor-infiltrating lymphocytes is associated with a favorable prognosis and response immunotherapy in cancer (7–9). We found that total counts of both CD4 and CD8 T cells were significantly decreased in *Kras/Lkb1* mouse tumors (Fig. 2A) as compared to *Kras* tumors. Infiltrating T cells showed a significantly higher expression of T cell inhibitory markers: Programmed cell death protein 1 (PD-1), T cell immunoglobulin mucin-3 (TIM-3), Lymphocyte-activation gene 3 (LAG-3) and cytotoxic T-lymphocyte-associated protein 4 (CTLA-4) (Fig. 2B). We also confirmed expression of the ligand for TIM-3, LGALS9, in both tumor cells and TAN from *Kras/Lkb1* tumors by flow cytometry (Supplementary Fig. S2D). The ratio of regulatory T cells ($FOXP3^+$) to total CD4 T cells was also significantly increased in *Kras/Lkb1* tumor as compared to *Kras* tumors (Fig. 2B). We evaluated T cell function in *Kras/Lkb1* and *Kras*

tumors with similar levels of disease (Supplementary Fig. S3B) and found significantly less IFNγ and Ki-67 expression in total CD4 and CD8 T cells from the *Kras/Lkb1* tumors than those from *Kras* tumors (Fig. 2C). Thus, *Lkb1* inactivation is associated with reduced T cell number and increased markers of T cell exhaustion.

To understand the role of neutrophils in this model, we used a neutrophil depleting (anti Ly-6G/Gr-1:RB6-8C5) antibody in mice with established tumors (Supplementary Fig. S4A and B). *Kras/Lkb1* mice treated with anti Ly-6G/Gr-1 antibody for 1 or 2 weeks showed a significant reduction of TAN and of IL-6 and G-CSF in BALFs (Supplementary Fig. S4C and D), resulting in a significant increase in total CD8 T cell numbers, proliferation ($Ki\text{-}67^+$) and T cell function represented by IFNγ production (Supplementary Fig. S4E).

PD-L1 expression on tumor cells is a biomarker associated with a response to PD-1 blockade treatment (7,10). *Lkb1*-deficient tumor cells expressed significantly lower levels of PD-L1 in $CD45^-EpCAM^+$ cells as compared to *Kras* tumor cells (Fig. 2D). PD-L1 expression is influenced by a variety of factors that include non-cell autonomous factors such as release of IFNγ from T cells (26) in the tumor microenvironment *in vivo.* To dissect the intrinsic role of *Lkb1* inactivation on PD-L1 expression specifically in tumor cells, we analyzed PD-L1 expression in cultured cell lines derived from mouse tumors of the KP and KPL genotypes. PD-L1 levels were significantly lower in KPL as compared to KP (Fig. 2E). To confirm that our findings in mouse models and cell lines were applicable to humans, we studied human lung cancer cell lines with endogenous *KRAS* mutation and wild type or inactivated *LKB1*. We either performed knockdown of *LKB1* using shRNA or reconstituted LKB1 with wild type (WT) or kinase dead (KD) LKB1 to develop isogenic cell lines (wild type cells: H441, H1792 and *LKB1* mutant cell: A549) (Supplementary Fig. S5A). PD-L1 expression was lower in both of the LKB1 WT lines when expressing sh-LKB1 (Fig. 2F). Expression of *LKB1* (WT and KD) in the *LKB1*-deficient A549 cell line resulted in a modest increase in PD-L1 levels (Supplementary Fig. S5B). These data suggest *LKB1* inactivation decreased PD-L1 levels independent of IFNγ.

Functional loss of *LKB1* in human cell lines is phenotypically similar to mouse *Kras/Lkb1* tumors

We next assessed the cytokine and chemokine profiles in human isogenic cell lines to determine whether similar patterns would be observed. We analyzed culture supernatants from these cell lines and found that IL-6 and G-CSF were significantly increased in *LKB1*-inactivated cells as compared to *LKB1*-intact cells (Fig. 3A and Supplementary Fig. S5C). There was also a significant increase of CXCL7 that was only detected in A549 cells (Supplementary Fig. S5C). IL-1α stimulation of these cell lines led to an increase in IL-6, G-CSF and CXCL7 in a dose-dependent manner (Fig. 3B and Supplementary Fig. S5D), which was consistent with the *Lkb1*-deficient mouse cell line data (Fig. 1D). We also found that IL-6 induction by IL-1α stimulation was more pronounced in *LKB1*-deficient cell lines as compared to *LKB1*-intact cell lines (Supplementary Fig. S5E) except for H1792 which showed modest stimulation. This line has high baseline IL-1α production (Fig. 3A) and the shRNA only partially knocked down *LKB1* (Supplementary Fig. S5A) which makes this result difficult to interpret.

Analysis of lung cancer cell lines from The Cancer Cell Line Encyclopedia (CCLE) (27) confirmed that PD-L1 expression is significantly lower in cell lines with *LKB1* mutation (32 *LKB1* WT and 4 *LKB1* mutant cell lines) (Fig. 3C), though the small number of *LKB1* mutant lines precluded any significant associations among the immune related genes displayed in Figures 1C and S2A and *LKB1* status when corrected for multiple hypotheses. In addition, analysis of *KRAS*-mutated lung adenocarcinomas from The Cancer Genome Atlas (TCGA-52 *LKB1* WT, 15 *LKB1* mutant) (2) showed that PD-L1 expression was significantly reduced in *LKB1*-mutated NSCLCs (Fig. 3C). In a multivariate analysis of the TCGA dataset with respect to *LKB1* status and clinical factors, PD-L1 and *LKB1* status were also significantly associated (p=0.005). To validate these findings in an independent dataset, PD-L1 mRNA was assessed in the MD Anderson PROSPECT (Profiling of Resistance Patterns and Oncogenic Signaling Pathways in Evaluation of Cancers of the Thorax and Therapeutic Target Identification) cohort (MDACC-108 *LKB1* WT, 44 *LKB1* MUTANT cases). We again observed an association among PD-L1 expression and *LKB1* status. We also validated and quantitated the expression of PD-L1 at the protein level by reverse phase protein arrays (RPPA) in 106 cases from the MDACC cohort and detected significantly lower levels of PD-L1 in *LKB1* mutant tumors (Fig. 3D). As the current clinical standard detection method for the PD-L1 expression is immunohistochemistry, we confirmed the difference in PD-L1 expression by immunohistochemistry (Fig. 3E).

Next, to evaluate the functional effect of *LKB1*-loss in the tumor microenvironment in patient tumors, we analyzed the T cell infiltrate in the tumors by immunohistochemistry. In 19 *LKB1* WT and 11 *LKB1* mutant tumors, total T cell ($CD3^+$) and CD8 T cell counts and densities were significantly lower in *LKB1*-inactivated tumors as compared to *LKB1*-intact tumors (Fig. 3F), In sum, observations in patient cell lines and tumor samples are consistent with our findings in *Kras/Lkb1* mice, suggesting that *LKB1* mutation negatively regulates PD-L1 expression and reduces CD8 T cell infiltration.

Neutralizing IL-6 leads to a therapeutic benefit in *Kras/Lkb1* mice

Supporting the notion that PD-L1 expression in tumor cells is critical in the response to PD-1 blockade, treatment of the *Kras/Lkb1* mouse model with a PD-1 blocking antibody did not show a significant treatment response (Fig. 4A). Given our observation of elevated IL-1α and IL-6 in BALFs (Fig. 1E and G) and aberrant activation of pSTAT3 in tumor nodules (Fig. 1F) from *Kras/Lkb1* mice as compared to *Kras* mice, we hypothesized that targeting aberrant cytokine production could be a rational therapeutic strategy in *Kras/Lkb1* mutant tumors. To evaluate in vivo efficacy of IL-6 blockade, we treated *Kras/Lkb1* mice with a neutralizing IL-6 antibody (MP5-20F3). The therapeutic anti IL-6 antibody significantly inhibited tumor progression as compared to anti PD-1 antibody (Fig. 4A). In addition, IL-6 antibody treated mice showed significantly improved survival as compared to control mice (Fig. 4B). However, treatment of *Kras/Lkb1* tumors with other checkpoint blocking antibodies against CTLA-4 or a combination of PD-1 and TIM-3 also did not demonstrate any efficacy (data not shown). Taken together, these findings suggest that *Lkb1*-loss results in a T cell suppressed environment as a consequence of autocrine and neutrophil induced cytokine production and not engagement of the PD-L1:PD-1 immune checkpoint.

To further investigate the effect of IL-6 neutralizing antibody on the immune profile of *Kras/Lkb1* tumors, we treated the mice for 2 weeks and then performed immune and histological analyses (Supplementary Fig. S6A). There was a significant reduction in detectable IL-6 as expected as well as G-CSF in BALFs from the treated mice (Fig. 4C). In keeping with the neutrophil attracting cytokines and chemokines observed in BALFs, there was a significant reduction in the counts of total TAN with IL-6 neutralization (Fig. 4D), resulting in functional recovery of T cells (Fig. 4E). Treated tumors also exhibited elevation of CD4 T cells, CD8 T cells, and TAM to levels that are comparable to *Lkb1* wild type tumors (Supplementary Fig. S6B). In addition to the immune related effects, IL-6 antibody treated tumor cells exhibited significantly less proliferation and increased apoptosis (Fig. 4F). Although therapeutic IL-6 blockade improved T cell function, concurrent therapy combining anti IL-6 and PD-1 treatment did not demonstrate additional benefit as compared to IL-6 blockade alone in terms of survival (Supplementary Fig. S6C). This suggests a need to further define contexts in which cytokine suppression and immune checkpoint blockade might be utilized together to enhance therapeutic benefit as compared to either treatment alone.

Discussion

Oncogenes and tumor suppressors promote self-sufficient signaling for autonomous proliferation of tumor cells. Recent work has shown that oncogenic mutations alter the tumor microenvironment, cause immune suppression and can impact the response to immune modulating treatment strategies (10). Somatic mutations also produce neo-antigens which are recognized by the immune system and mediate sensitivity of the tumors to immunotherapies (28–30). Here, we have shown that inactivation of the tumor-suppressor gene *STK11*/*LKB1* causes dramatic changes in the tumor microenvironment in addition to the previously reported effects on cell cycle, metabolism, differentiation, polarity and other cellular pathways (16,31).

We have shown that *LKB1* inactivation promoted the production of proinflammatory cytokines CXCL7, G-CSF and IL-6 in both mouse tumors and cell lines, which contributes to neutrophil accumulation. Elevation of the proinflammatory cytokine IL-1α was confirmed *in vivo* but not robustly in cell culture supernatants from *Lkb1*-deficient cells. Previous studies have shown that IL-1α is released only under specific conditions including necrotic cell death and inflammasome activation (32,33), suggesting that the release of IL-1α could be caused by necrotic cell death in *Kras/Lkb1* tumor microenvironment and that this facilitates the activation of IL-6-STAT3 signaling pathway in *Kras/Lkb1* tumors together with IL-6, producing neutrophil accumulation.

The tumor microenvironment in *Kras/Lkb1* tumors displayed characteristics of T cell suppression with fewer lymphocytes, higher levels of checkpoint receptor expression in those, and an increase in TANs with suppressive properties compared to *Kras* tumors. TANs expressing high levels of *Il10, Arginase1* and *Mfge8* that have been implicated in T cell suppression and Treg induction (15,22,34). Depleting TAN using an anti Ly-6G/Gr-1 antibody improved T cell function. Although the role of TAN in suppressing T cell function is controversial (35), TAN appear to act in an immunosuppressive fashion in this context,

suggesting that therapies suppressing TAN should be further explored as immunomodulatory therapies.

Moreover, we found that *Lkb1* inactivation caused a decrease in PD-L1 levels on tumor cells from *Kras/Lkb1* tumors and in cultured cells from mice and patients. Conforming to the previous observations proposing an association of tumor cell PD-L1 expression, the magnitude of T cell accumulation in the tumors and response to PD-1 blockade (7,8,36), treatment with a PD-1 blocking antibody did not show efficacy in the treatment of the *Kras/Lkb1* mouse model. A recent study (30) as well as our own institutional experience suggest that while *KRAS* mutated patients respond favorably to PD-1 blockade (PFS of 15 months on pembrolizumab) this is not seen in patients with *LKB1* mutations though large cohorts will be needed to define genotype-response associations in detail. Additionally contributing to low PD-1:PD-L1 levels in *Kras/Lkb1* tumors is the greater proportion of TAN which express low levels of PD-L1 as compared to TAM. The coordinated role of PD-L1 expression in the tumor cells and the cells constituting the immune microenvironment in this model requires further study to define improved immunotherapeutic strategies.

Treatment of *Kras/Lkb1* tumors with an IL-6 blocking antibody decreased tumor cell proliferation and increased T cell function, resulting in a therapeutic effect in *Kras/Lkb1* mouse model while immune checkpoint blockade was not efficacious. These data suggest that mouse models can be used to model the tumor microenvironment and predict response to novel immune modulating treatment strategies based on rational predictions from studies of the tumor microenvironment. Future studies will examine whether cytokines other than IL-6 also contribute to STAT3 activation (37), and whether combined cytokine blockade (e.g, with IL-1 neutralization) will lead to more durable therapeutic effects. Although we found that neutralizing IL-6 antibodies improved T cell number and function in Lkb1-deficient tumors, the combination of anti PD-1 plus anti IL-6 antibodies did not improve outcome when given concurrently. There may be technical limitations to this considering both of the antibodies are Rat IgG isotype and combination treatment can lead to antibody neutralization. Further, dosing schedules of cytokine suppression and combinations with other therapeutic agents such as immune checkpoint blockade will need to be studied.

In summary, we have presented a novel set of findings which suggest that not only oncogene driver mutations but also tumor-suppressor gene mutations can modify the immune microenvironment in lung cancer. In this example focusing on *Lkb1* loss we observed a marked increase in inflammatory cytokines that recruited neutrophils and inhibited the function of T cells. We also showed that PD-1 checkpoint blockade was ineffective in *Lkb1* mutant cancers, whereas targeting IL-6 displayed a significant albeit short-lived treatment response in the *Kras/Lkb1* model. These findings suggest that IL-6 dependent signaling activation can be a therapeutic target in *Lkb1* deficient *Kras*-driven lung tumors and potentially other tumors with high levels of IL-6, and also suggest targeting aberrant inflammation by inhibiting cytokine signaling may represent a promising immunotherapeutic strategy in selected patients.

Supplementary Material

Refer to Web version on PubMed Central for supplementary material.

Acknowledgments

The authors thank Suzan Lazo-Kallanian, John Daley, Kristen Cowens and Steven Paul for help with flow cytometry anlaysis, Christine Lam for tissue processing, Mei Zhang for immunohistochemistry, Xiaoen Wang for helping with mouse studies, and the Dana Farber Center for Cancer Genome Discovery for RNA sequencing.

Financial support

P.S.H. is supported by a Clinical Investigator Award from the Damon Runyon Cancer Research Foundation and the Starr Consortium for Cancer Research. P.S.H., K.K.W., J.V.H. and M.D.H. are supported by a Stand Up To Cancer - American Cancer Society Lung Cancer Dream Team Translational Research Grant (Grant Number: SU2C-AACR-DT17-15). Stand Up To Cancer is a program of the Entertainment Industry Foundation. Research grants are administered by the American Association for Cancer Research, the scientific partner of SU2C. K.K.W. is supported by NCI R01 CA195740. S.K. is supported by Margaret A. Cunningham Immune Mechanisms in Cancer Research Fellowship Award and The Kanae Foundation for the Promotion of Medical Science Fellowship Award. G.S.H.-S. was supported by the Deutsche Forschungsgemeinschaft (HE 6897/1-1) and the Claudia Adams Barr Program for Innovative Cancer Research. T.S. is supported by Uniting Against Lung Cancer Legacy Program and American Cancer Society Research Scholar Award.

References

1. Cardarella S, Johnson BE. The impact of genomic changes on treatment of lung cancer. American journal of respiratory and critical care medicine. 2013; 188(7):770–5. [PubMed: 23841470]
2. Comprehensive molecular profiling of lung adenocarcinoma. Nature. 2014; 511(7511):543–50. [PubMed: 25079552]
3. Ji H, Ramsey MR, Hayes DN, Fan C, McNamara K, Kozlowski P, et al. LKB1 modulates lung cancer differentiation and metastasis. Nature. 2007; 448(7155):807–10. [PubMed: 17676035]
4. Chen Z, Cheng K, Walton Z, Wang Y, Ebi H, Shimamura T, et al. A murine lung cancer co-clinical trial identifies genetic modifiers of therapeutic response. Nature. 2012; 483(7391):613–7. [PubMed: 22425996]
5. Zhao N, Wilkerson MD, Shah U, Yin X, Wang A, Hayward MC, et al. Alterations of LKB1 and KRAS and risk of brain metastasis: Comprehensive characterization by mutation analysis, copy number, and gene expression in non-small-cell lung carcinoma. Lung cancer (Amsterdam, Netherlands). 2014
6. Calles A, Sholl LM, Rodig SJ, Pelton AK, Hornick JL, Butaney M, et al. Immunohistochemical loss of LKB1 is a biomarker for more aggressive biology in KRAS mutant lung adenocarcinoma. Clinical cancer research : an official journal of the American Association for Cancer Research. 2015
7. Taube JM, Klein A, Brahmer JR, Xu H, Pan X, Kim JH, et al. Association of PD-1, PD-1 Ligands, and Other Features of the Tumor Immune Microenvironment with Response to Anti-PD-1 Therapy. Clinical cancer research : an official journal of the American Association for Cancer Research. 2014; 20(19):5064–74. [PubMed: 24714771]
8. Tumeh PC, Harview CL, Yearley JH, Shintaku IP, Taylor EJ, Robert L, et al. PD-1 blockade induces responses by inhibiting adaptive immune resistance. Nature. 2014; 515(7528):568–71. [PubMed: 25428505]
9. Herbst RS, Soria JC, Kowanetz M, Fine GD, Hamid O, Gordon MS, et al. Predictive correlates of response to the anti-PD-L1 antibody MPDL3280A in cancer patients. Nature. 2014; 515(7528): 563–7. [PubMed: 25428504]
10. Akbay EA, Koyama S, Carretero J, Altabef A, Tchaicha JH, Christensen CL, et al. Activation of the PD-1 pathway contributes to immune escape in EGFR-driven lung tumors. Cancer discovery. 2013; 3(12):1355–63. [PubMed: 24078774]

11. Ochoa CE, Mirabolfathinejad SG, Ruiz VA, Evans SE, Gagea M, Evans CM, et al. Interleukin 6, but not T helper 2 cytokines, promotes lung carcinogenesis. Cancer prevention research (Philadelphia, Pa). 2011; 4(1):51–64.
12. Ancrile B, Lim KH, Counter CM. Oncogenic Ras-induced secretion of IL6 is required for tumorigenesis. Genes & development. 2007; 21(14):1714–9. [PubMed: 17639077]
13. Barbie DA, Tamayo P, Boehm JS, Kim SY, Moody SE, Dunn IF, et al. Systematic RNA interference reveals that oncogenic KRAS-driven cancers require TBK1. Nature. 2009; 462(7269): 108–12. [PubMed: 19847166]
14. Meylan E, Dooley AL, Feldser DM, Shen L, Turk E, Ouyang C, et al. Requirement for NF-kappaB signalling in a mouse model of lung adenocarcinoma. Nature. 2009; 462(7269):104–7. [PubMed: 19847165]
15. Motz GT, Coukos G. Deciphering and reversing tumor immune suppression. Immunity. 2013; 39(1):61–73. [PubMed: 23890064]
16. Liu Y, Marks K, Cowley GS, Carretero J, Liu Q, Nieland TJ, et al. Metabolic and functional genomic studies identify deoxythymidylate kinase as a target in LKB1-mutant lung cancer. Cancer discovery. 2013; 3(8):870–9. [PubMed: 23715154]
17. Shimamura T, Chen Z, Soucheray M, Carretero J, Kikuchi E, Tchaicha JH, et al. Efficacy of BET bromodomain inhibition in Kras-mutant non-small cell lung cancer. Clinical cancer research : an official journal of the American Association for Cancer Research. 2013; 19(22):6183–92. [PubMed: 24045185]
18. Zhu Z, Aref AR, Cohoon TJ, Barbie TU, Imamura Y, Yang S, et al. Inhibition of KRAS-driven tumorigenicity by interruption of an autocrine cytokine circuit. Cancer discovery. 2014; 4(4):452–65. [PubMed: 24444711]
19. Tchaicha JH, Akbay EA, Altabef A, Mikse OR, Kikuchi E, Rhee K, et al. Kinase domain activation of FGFR2 yields high-grade lung adenocarcinoma sensitive to a Pan-FGFR inhibitor in a mouse model of NSCLC. Cancer research. 2014; 74(17):4676–84. [PubMed: 25035393]
20. Franciszkiewicz K, Boutet M, Gauthier L, Vergnon I, Peeters K, Duc O, et al. Synaptic release of CCL5 storage vesicles triggers CXCR4 surface expression promoting CTL migration in response to CXCL12. J Immunol. 2014; 193(10):4952–61. [PubMed: 25305322]
21. Luther SA, Bidgol A, Hargreaves DC, Schmidt A, Xu Y, Paniyadi J, et al. Differing activities of homeostatic chemokines CCL19, CCL21, and CXCL12 in lymphocyte and dendritic cell recruitment and lymphoid neogenesis. J Immunol. 2002; 169(1):424–33. [PubMed: 12077273]
22. Najjar YG, Finke JH. Clinical perspectives on targeting of myeloid derived suppressor cells in the treatment of cancer. Frontiers in oncology. 2013; 3:49. [PubMed: 23508517]
23. Walker F, Zhang HH, Matthews V, Weinstock J, Nice EC, Ernst M, et al. IL6/sIL6R complex contributes to emergency granulopoietic responses in G-CSF- and GM-CSF-deficient mice. Blood. 2008; 111(8):3978–85. [PubMed: 18156493]
24. Suzuki E, Mellins ED, Gershwin ME, Nestle FO, Adamopoulos IE. The IL-23/IL-17 axis in psoriatic arthritis. Autoimmunity reviews. 2014; 13(4–5):496–502. [PubMed: 24424175]
25. Leslie K, Gao SP, Berishaj M, Podsypanina K, Ho H, Ivashkiv L, et al. Differential interleukin-6/Stat3 signaling as a function of cellular context mediates Ras-induced transformation. Breast cancer research : BCR. 2010; 12(5):R80. [PubMed: 20929542]
26. Rodig N, Ryan T, Allen JA, Pang H, Grabie N, Chernova T, et al. Endothelial expression of PD-L1 and PD-L2 down-regulates CD8+ T cell activation and cytolysis. European journal of immunology. 2003; 33(11):3117–26. [PubMed: 14579280]
27. Barretina J, Caponigro G, Stransky N, Venkatesan K, Margolin AA, Kim S, et al. The Cancer Cell Line Encyclopedia enables predictive modelling of anticancer drug sensitivity. Nature. 2012; 483(7391):603–7. [PubMed: 22460905]
28. Gubin MM, Zhang X, Schuster H, Caron E, Ward JP, Noguchi T, et al. Checkpoint blockade cancer immunotherapy targets tumour-specific mutant antigens. Nature. 2014; 515(7528):577–81. [PubMed: 25428507]
29. Yadav M, Jhunjhunwala S, Phung QT, Lupardus P, Tanguay J, Bumbaca S, et al. Predicting immunogenic tumour mutations by combining mass spectrometry and exome sequencing. Nature. 2014; 515(7528):572–6. [PubMed: 25428506]

30. Rizvi NA, Hellmann MD, Snyder A, Kvistborg P, Makarov V, Havel JJ, et al. Cancer immunology. Mutational landscape determines sensitivity to PD-1 blockade in non-small cell lung cancer. Science (New York, NY). 2015; 348(6230):124–8.

31. Skoulidis F, Byers LA, Diao L, Papadimitrakopoulou VA, Tong P, Izzo J, et al. Co-occurring Genomic Alterations Define Major Subsets of KRAS-Mutant Lung Adenocarcinoma with Distinct Biology, Immune Profiles, and Therapeutic Vulnerabilities. Cancer discovery. 2015; 5(8):860–77. [PubMed: 26069186]

32. Chen GY, Nunez G. Sterile inflammation: sensing and reacting to damage. Nature reviews Immunology. 2010; 10(12):826–37.

33. Voronov E, Dotan S, Krelin Y, Song X, Elkabets M, Carmi Y, et al. Unique Versus Redundant Functions of IL-1alpha and IL-1beta in the Tumor Microenvironment. Frontiers in immunology. 2013; 4:177. [PubMed: 23847618]

34. Jinushi M, Hodi FS, Dranoff G. Enhancing the clinical activity of granulocyte-macrophage colony-stimulating factor-secreting tumor cell vaccines. Immunological reviews. 2008; 222:287–98. [PubMed: 18364009]

35. Eruslanov EB, Bhojnagarwala PS, Quatromoni JG, Stephen TL, Ranganathan A, Deshpande C, et al. Tumor-associated neutrophils stimulate T cell responses in early-stage human lung cancer. The Journal of clinical investigation. 2014; 124(12):5466–80. [PubMed: 25384214]

36. Garon EB, Rizvi NA, Hui R, Leighl N, Balmanoukian AS, Eder JP, et al. Pembrolizumab for the treatment of non-small-cell lung cancer. The New England journal of medicine. 2015; 372(21): 2018–28. [PubMed: 25891174]

37. Yu H, Pardoll D, Jove R. STATs in cancer inflammation and immunity: a leading role for STAT3. Nature reviews Cancer. 2009; 9(11):798–809. [PubMed: 19851315]

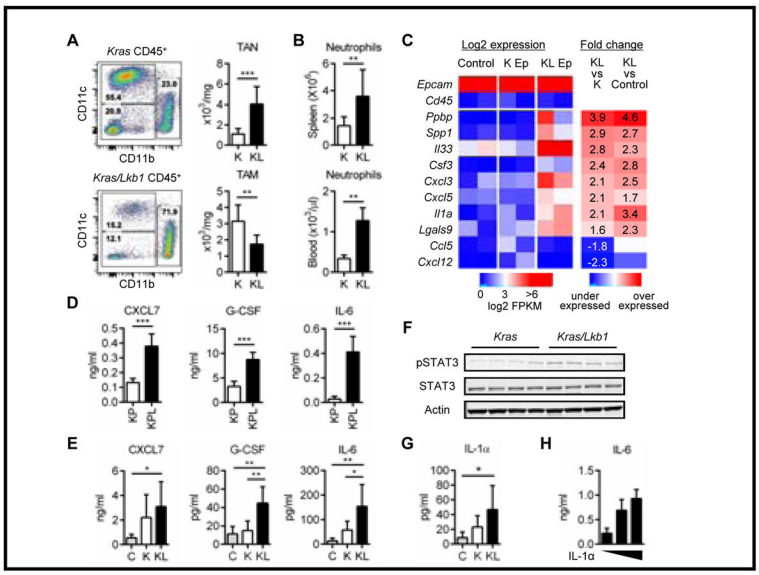

Figure 1. Tumor-suppressor *Lkb1* inactivation promotes neutrophil accumulation via proinflammatory cytokines and chemokines

A. Immune cell populations in the lung tumors from *Kras* (K) and *Kras/Lkb1* (KL) mouse models. Representative flow cytometry data (live/single/total $CD45^+$ cells) from each mouse model (left). Total counts of tumor associated neutrophils (TAN): $CD11b^+Ly\text{-}6G^+$ cells and tumor associated macrophages (TAM): $CD11c^+CD11b^-CD103^-$ from K (n=8) and KL (n=8) mice. **p<0.01, ***p<0.001. **B**. Neutrophil counts in the spleen and peripheral blood from K (n=8) or KL (n=8) mice (right). **p<0.01. **C**. Expression of immune modulating factors from RNA sequencing of the sorted tumor cells ($CD45^-EpCAM^+$) in *Kras* (K Ep) or *Kras/Lkb1* (*KL* Ep) mice and uninduced normal lung $CD45^-EpCAM^+$ cells (Control). Each column consists of a combination of samples derived from 3–4 mice. Log-transformed FPKM values are shown, colored blue/red for low/high expression, respectively. *Epcam* and *Cd45* expression are shown as positive and negative controls. Differential expression is shown as fold-change values, colored blue/red for under/over-expression compared to controls. **D, E**. Chemokine and cytokine levels in the culture supernatants after 48hr incubation from *Kras/p53* (KP) (n=3) versus *Kras/p53/Lkb1* (KPL) (n=3) cell lines generated from mouse lung tumors, ***p<0.001. Data indicate three replicate wells and are representative of three independent experiments (D) and bronchoalveolar lavage fluid (BALF)s from littermate controls (n=5), K mice (n=8) or KL mice (n=8). *p<0.05, **p<0.01 (E). **F**. Western blot analysis for pSTAT3, STAT3 levels in K versus KL tumors. Each column represents tumor from a different mouse and actin represents loading control. **G**. IL-1α level in the BALF from C (n=5), K (n=8) or KL (n=8) mice. *p<0.05. **H**. IL-6 levels in culture supernatants measured 24hr after IL-1α stimulation (0, 5 and 20ng/ml) of KP (n=3) versus KPL (n=3) cell lines. Data indicate three replicate wells and are representative of three independent experiments.

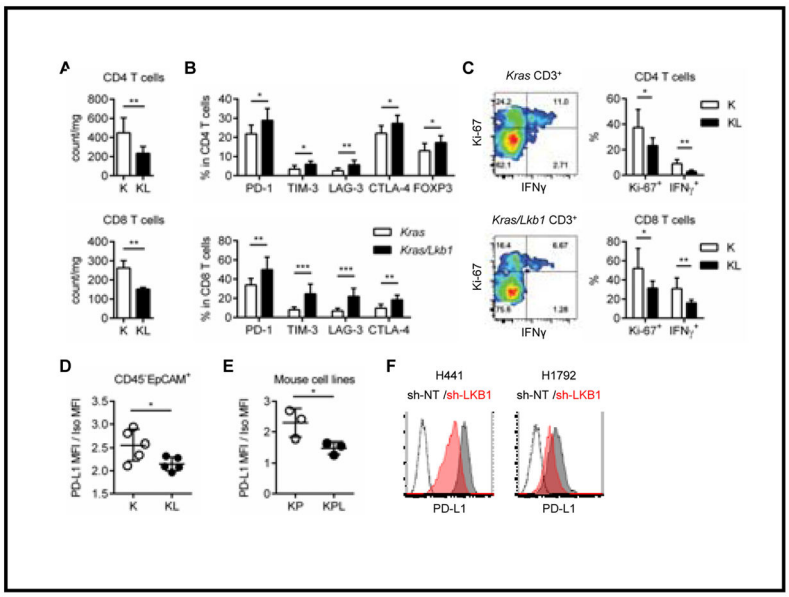

Figure 2. *Lkb1* inactivation leads to a T cell suppressive tumor microenvironment with low PD-L1 expression in tumor cells

A. Total counts of CD4 T cells (top) and CD8 T cells (bottom). **p<0.01. **B**. Expression of checkpoint receptors in CD4 T cells (top) and CD8 T cells (bottom) in K or KL tumors. *p<0.05, **p<0.01, ***p<0.001. **C**. IFNγ expression and proliferation marker (Ki-67) positivity for CD4 or CD8 T cells in K or KL tumors. Representative flow cytometry data (total $CD3^+$ T cells) from each mouse model (left). Percentage of $Ki\text{-}67^+$ and $IFN\gamma^+$ in CD4 or CD8 T cells from K (n=6) or KL (n=6) mice. *p<0.05, **p<0.01. **D**. PD-L1 expression in gated $CD45^-EpCAM^+$ cells in K (n=5) or KL (n=5) tumors evaluated by flow cytometry. *p=0.0384. **E**. PD-L1 expression in KP (n=3) versus KPL (n=3) cell lines evaluated by flow cytometry. *p=0.0495. Data is representative of three independent experiments. **F**. PD-L1 expression in H441 or H1792 cells stably transfected with sh-non-target (NT) or sh-LKB1. Data are representative of three independent experiments.

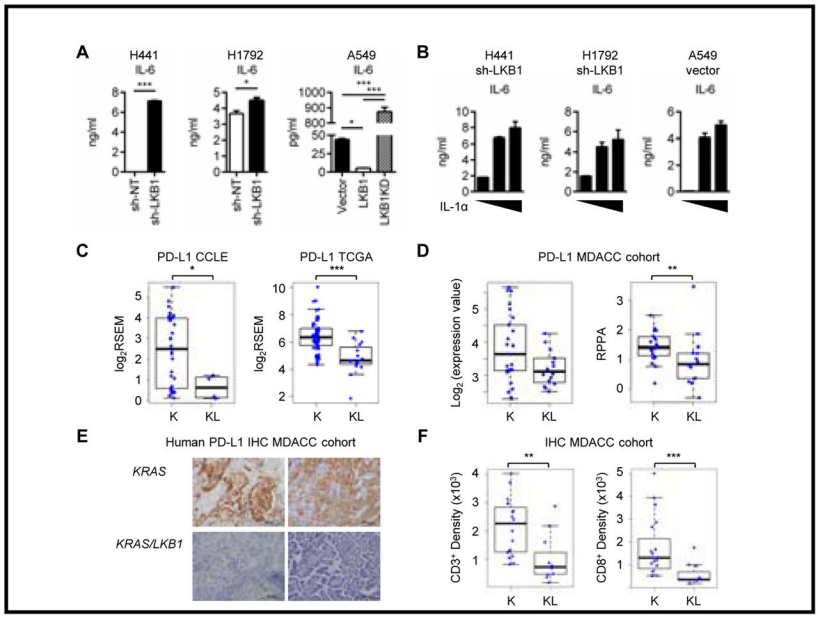

Figure 3. *LKB1* inactivation in human *KRAS* mutated cell lines showed similar phenotype with mouse *Kras/Lkb1* tumor

A. Analysis of IL-6 in the culture supernatants after 48hr incubation of *KRAS* mutated *LKB1* wild type H441 or H1792 cells stably transfected with sh-NT or sh-LKB1 and *KRAS*, *LKB1* mutant A549 cells reconstituted with empty vector (Vector), wild type LKB1 or Kinase dead LKB1 (LKB1KD). *p<0.05, ***p<0.001. Data indicate three replicate wells and are representative of three independent experiments. **B**. IL-6 levels in culture supernatants measured 24hr after IL-1α stimulation (0, 5 and 20ng/ml) of three *LKB1*-deficient cell lines. Data indicate three replicate wells and are representative of three independent experiments. **C**. *PDL1* expression in *KRAS* (K) or *KRAS* and *LKB1* mutated (KL) cell lines from CCLE database (*p=0.04) and *PDL1* expression in K or KL lung adenocarcinoma samples from TCGA database (***p=0.00004). **D.** *PD-L1* mRNA levels determined by microarray (p=0.1) and protein levels (**p=0.009) determined by RPPA from the MDACC dataset**. E.** Representative immunohistochemistry for PD-L1 on the *KRAS* mutated *LKB1* wt or mutant patient tumors from the MDACC cohort. **F.** CD3 (**p=0.002) and CD8 (***p=0.0003) positive cell densities by immunohistochemistry on the MDACC patient cohorts.

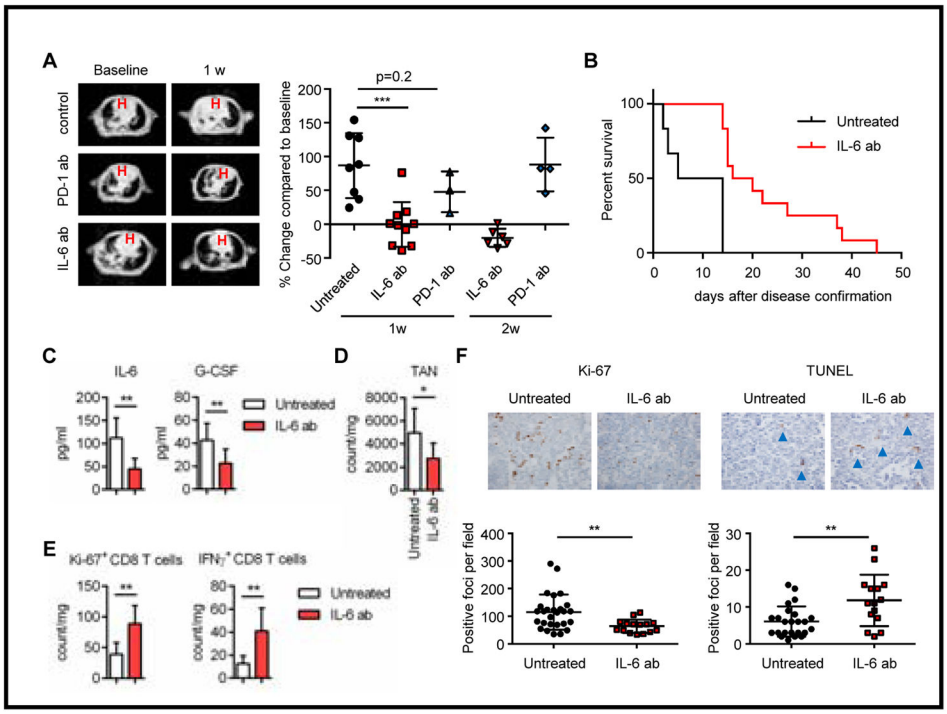

Figure 4. IL-6 neutralizing treatment showed clinical efficacy in *Kras/Lkb1* mouse model

A. Representative images of Magnetic resonance imaging (MRI) and quantification of MRI from KL mice treated with PD-1 or IL-6 blocking antibodies or controls. **B**. Survival of untreated mice vs mice treated with IL-6 blocking antibody (***p=0.0002, n=6 vs 12 respectively). **C, D**. IL-6 and G-CSF levels in BALFs (C) and TAN counts (D) for untreated KL mice (n=7) or KL mice treated with IL-6 neutralizing antibody (n=8) with comparable tumor burden. *p<0.05, **p<0.01. **E.** Ki-67 and IFNγ positive CD8 T cell counts in untreated KL mice (n=7) or KL mice treated with IL-6 neutralizing antibody (n=8) with comparable tumor burden. **F**. Representative Ki-67 and TUNEL immunohistochemistry and quantification per the microscopic field on the KL mice untreated or treated with IL-6 neutralizing antibody. Each data point represents a different microscopic field. For Ki-67 n=9 and 5 and for TUNEL n=8 and 5 for untreated and IL-6 ab treated mice respectively. **p=0.0049 for Ki-67 and **p=0.0024 for TUNEL.